analytical chemistry

Article

pubs.acs.org/ac

Structural Resolution of 4-Substituted Proline Diastereomers with Ion Mobility Spectrometry via Alkali Metal Ion Cationization

Tawnya G. Flick,*[,†] Iain D. G. Campuzano,[‡] and Michael D. Bartberger[‡]

[†]Department of Oral Attribute Sciences, Amgen, Inc., Thousand Oaks, California 91320, United States

[‡]Department of Molecular Structure and Characterization, Amgen, Inc., Thousand Oaks, California 91320, United States

Supporting Information

ABSTRACT: The chirality of substituents on an amino acid can significantly change its mode of binding to a metal ion, as shown here experimentally by traveling wave ion mobility spectrometry-mass spectrometry (TWIMS-MS) of different proline isomeric molecules complexed with alkali metal ions. Baseline separation of the *cis*- and *trans*- forms of both hydroxyproline and fluoroproline was achieved using TWIMS-MS via metal ion cationization (Li^+, Na^+, K^+, and Cs^+). Density functional theory calculations indicate that differentiation of these diastereomers is a result of the stabilization of differing metal-complexed forms adopted by the diastereomers when cationized by an alkali metal cation, $[M + X]^+$ where X = Li, Na, K, and Cs, versus the topologically similar structures of the protonated molecules, $[M + H]^+$. Metal-cationized *trans*-proline variants exist in a linear salt-bridge form where the metal ion interacts with a deprotonated carboxylic acid and the proton is displaced onto the nitrogen atom of the pyrrolidine ring. In contrast, metal-cationized *cis*-proline variants adopt a compact structure where the carbonyl of the carboxylic acid, nitrogen atom, and if available, the hydroxyl and fluorine substituent solvate the metal ion. Experimentally, it was observed that the resolution between alkali metal-cationized *cis*- and *trans*-proline variants decreases as the size of the metal ion increases. Density functional theory demonstrates that this is due to the decreasing stability of the compact charge-solvated *cis*-proline structure with increased metal ion radius, likely a result of steric hindrance and/or weaker binding to the larger metal ion. Furthermore, the unique structures adopted by the alkali metal-cationized *cis*- and *trans*-proline variants results in these molecules having significantly different quantum mechanically calculated dipole moments, a factor that can be further exploited to improve the diastereomeric resolution when utilizing a drift gas with a higher polarizability constant.

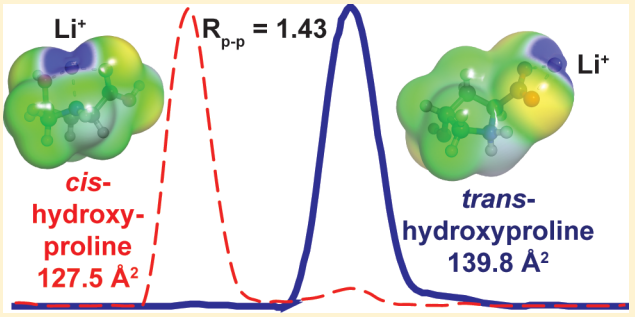

The development of analytical methods for differentiating chirality in molecules has been a major focus of separation chemistry for a wide range of applications, including those in drug discovery[1,2] and proteomics.[3−5] In drug discovery, molecular chirality is a major focus because most small organic compounds have enantiomeric forms, and these forms can differ in toxicity and activity in biological systems.[1,2] Also, changes in chirality of single amino acids in the primary sequence of peptides and large proteins can have a significant impact on higher-order structure.[3−8] Typically, chiral separations are achieved via liquid or gas chromatography, but optimizations and analysis using these separations can often be long and tedious.[9−11] In an effort to eliminate these slow and tedious steps, there has been significant interest in the development of methods that enable chiral discrimination in mass spectrometry (MS).[12−37] However, isomeric species have the same exact mass, making it impossible to differentiate these ions by m/z alone. Therefore, several mass spectrometric strategies for distinguishing isomeric species using mass spectrometry have been developed, including the kinetic method based on the dissociation of cluster ions,[12,22] collision-induced dissociation of diastereomeric adducts,[23,27] host−guest ion molecule reactions,[23−26,28,29] and ion mobility analysis.[12−20,30−37]

Ion mobility spectrometry (IMS) has the ability to rapidly separate isomeric species based on their mobilities through a drift gas under the influence of an electric field, which depends primarily on the shape and charge of the gas-phase ion. The IMS-MS combination has therefore provided a proven mechanism for the gas-phase separation and characterization of isomers and conformers ranging from small molecules[31,33,36,38] and amino acids[16,33,39] to proteins[40−42] and large native protein complexes.[42−44] In traveling wave ion mobility spectrometry (TWIMS)-MS, a wave of amplitude V is applied to a set of adjacent pairs of lenses and moved along the mobility cell at a velocity v. Compared to static field IMS devices, this device has high transmission efficiency but suffers from lower resolution.[45,46] Recently, several strategies have

Received: November 19, 2014
Accepted: February 9, 2015
Published: February 9, 2015

DOI: 10.1021/ac5043285
Anal. Chem. 2015, 87, 3300−3307

been reported that can be used to increase the resolution between isomers using IMS-MS, including addition of a chiral modifier in the drift gas,[17,38] varying the drift gas,[19,20,34,35] metal ion adduction,[14,32] and complex dimer formation.[14] A pair of constitutional isomers, N-butylaniline and para-butylaniline, with theoretical collisional cross sections (ccs: Ω) that differ by 1.2 Å^2 show baseline resolution using a TWIMS-MS instrument for the protonated ion using carbon dioxide, nitrous oxide, and ethene as the drift gas.[19] Hill and co-workers also demonstrated that two enantiomers, (*S*)-atenolol and (*R*)-atenolol, using atmospheric pressure IM can be resolved in the gas phase when the drift gas in the ion mobility cell is modified with a chiral vapor.[38] More recently, the formation of multimers and metal ion adducts to diastereomeric small molecules was used to improve the isomeric resolution observed in TWIMS-MS experiments.[14,32]

Stabilization of salt-bridge and charge-solvated amino acid geometries in the gas phase with alkali metal ions has been extensively studied with infrared multiple photon dissociation (IRMPD) spectroscopy, and metal ion size has been shown to be a significant factor in the stabilization of a given structure.[47−56] While IRMPD has been the primary tool to evaluate amino acid gas-phase geometries in the past, it is particularly interesting to investigate whether salt-bridge or charge-solvated forms for different isomeric species can be elucidated with TWIMS analysis. Here, we report the TWIMS spectra of protonated and alkali metal-cationized *cis*- and *trans*-proline variants and results of complementary density functional theory calculations in combination with a nitrogen-based trajectory method (TM) algorithm that explores a wide range of salt-bridge and charge-solvated structures. Furthermore, the effect of the drift gas polarizability on improving the resolution observed between the diastereomers is evaluated on TWIMS and an RF-confining drift cell instrument. These results show that the isomeric form of the proline variants dictates the gas-phase geometry adopted by the ion when adducted to an alkali metal ion and provides a possible route to resolving isomeric amino acids using TWIMS analysis.

EXPERIMENTAL SECTION

Sample Preparation. The *cis*- and *trans*- forms of 4-substituted hydroxyproline and fluoroproline were all purchased from Bachem (Torrance, CA, U.S.A.). The chloride salts of Na^+, Li^+, K^+, and Cs^+ and all calibrant ions (N-ethylaniline, acetaminophen, alprenolol, ondansetron, and clozapine N-oxide) were purchased from Sigma-Aldrich (St. Louis, MO). Calibrant solutions were prepared at a concentration of 1 μM for each calibrant in 49.5/49.5/1.0 water/acetonitrile/acetic acid. Sample solutions for analysis were prepared at a final concentration of 10 μM proline variant in purely aqueous solutions with and without 1 mM of a chloride salt.

Instrument Parameters for Ion Mobility Measurements. TWIMS experiments were performed using a Synapt G2 high definition mass spectrometer (HDMS), and RF-confining drift tube measurements were performed on a modified Synapt G1 HDMS (Waters, Milford, MA, U.S.A.) both operated in positive ESI mode. Further experimental details can be found in the Supporting Information.

Theoretical Studies. Exhaustive conformational ensembles of singly charged protonated and metalated molecules of *cis*-hydroxyproline, *trans*-hydroxyproline, *cis*-fluoroproline, *trans*-fluoroproline, and *trans*-proline were generated with the MMFF (molecular mechanics force field) and utilizing the low mode molecular dynamics (LMMD) search algorithm as implemented in the Molecular Operating Environment (MOE) program suite.[57] All resultant, structurally unique MMFF geometries were then optimized using the B3LYP functional and 6-31++G(d,p) basis set on all atoms except cesium, for which the pseudopotential-corrected SVPD basis of Rappoport et al. was employed.[58] Vibrational frequency analyses characterized all stationary points as minima and allowed for relative free energy determination. Electrostatic potential-derived charges were fit using the Merz−Singh−Kollman scheme[59] and constrained to reproduce the computed dipole moment. All quantum mechanical calculations utilized the Gaussian 09 program system.[60]

TM Calculations. The TM algorithm was originally developed by Jarrold and co-workers[61] and is based on an ion's neutral interaction with the drift gas He. Theoretical Ω_{N2} values were calculated using modified versions of the TM.[31] Additional modifications were also made due to the nature of the compounds investigated within this study. UFF values[62] of atomic distance (Å) and energy (meV) for lithium, potassium, and cesium were added to the TM code so the Lennard−Jones parameters could be approximated and representative Ω_{N2} values could be calculated. For the N_2 TM, a scaling factor of 0.93 was applied to the UFF lithium, potassium, and cesium values, resulting in atomic distance and energy values of 2.279 Å and 1.008 meV, 3.545 Å and 1.411 meV, and 4.201 Å and 1.815 meV, respectively. It is fully acknowledged within this study that the Lennard−Jones potential values for the atoms lithium, potassium, and cesium are approximations and may well lead to errors in the reported theoretical Ω_{N2} values. However, in the absence of accurate lithium, potassium, or cesium IM-derived Lennard−Jones values, our chosen values, based on scaled and previously published UFF values, appeared to be workable, and the theoretically calculated Ω_{N2} values were consistent with the calibrated TWIMS and RF-confining drift cell drift times. Assuming the geometries for each molecule are an ensemble of a Boltzmann energy distribution, a Ω_{N2} value was determined by weighting the Ω_{N2} for each geometry by their contributing population for structures that possess relative Gibbs free energies with values of 5 kcal mol^{-1} or less.

RESULTS AND DISCUSSION

Ion Mobility Spectra of *cis*- and *trans*-hydroxyproline and fluoroproline. ESI of an aqueous solution containing 1 mM NaCl and either *cis*- or *trans*-hydroxyproline results in singly charged protonated and sodiated monomers with identical *m*/*z* values for both diastereomers (Figure 1). Collision induced dissociation of $[M + H]^+$ and $[M + Na]^+$ results in similar fragmentation patterns (Figure S1), making it challenging to distinguish these diastereomers by MS or MS^n experiments alone. With the need for an orthogonal technique to differentiate these diastereomers, TWIMS-MS experiments were performed to investigate if protonated or sodiated ionic structures of these diastereomers can be distinguished by their Ω_{N2}. The drift time difference between the protonated ions of *cis*- and *trans*-hydroxyproline was determined to be 0.05 ms, corresponding to a 0.6 Å^2 difference in the experimental Ω_{N2} and a $R_{p\text{-}p}$ of 0.08 (Figure 2a). The Ω_{N2} of $[M + Na]^+$ for both *cis*- and *trans*-hydroxyproline is significantly larger than that observed for the corresponding protonated ions (Figure 2b). Interestingly, [*trans*-hydroxyproline + $Na]^+$ has a significantly larger Ω_{N2} than that observed for [*cis*-hydroxyproline + $Na]^+$. This results in a factor of about a 3.0 and 11.5 increase in the

DOI: 10.1021/ac5043285
Anal. Chem. 2015, 87, 3300−3307

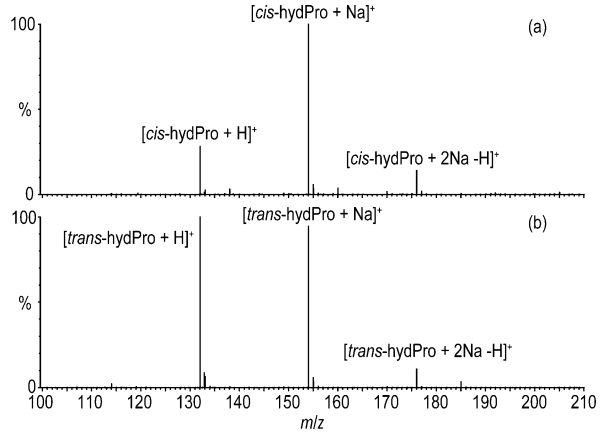

Figure 1. ESI mass spectra of 10 μM (a) *cis*- or (b) *trans*-hydroxyproline (hydPro) in a 1.0 mM NaCl aqueous solution.

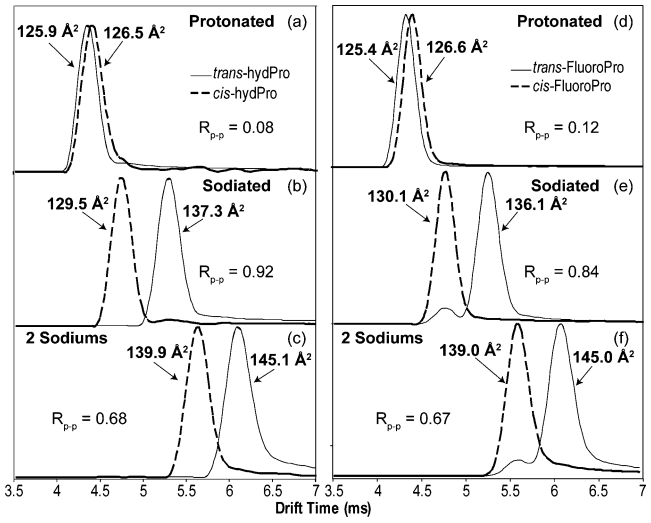

Figure 2. Traveling wave ion mobility spectra for (a, d) $[M + H]^+$, (b, e) $[M + Na]^+$, and (c, f) $[M + 2Na - H]^{2+}$ for *cis*- and *trans*- forms of hydroxyproline and fluoroproline, respectively, using N_2 as the drift gas.

Ω_{N2} difference and $R_{p\text{-}p}$ (0.92), respectively, between sodiated *cis*- and *trans*-hydroxyproline compared to the protonated counterparts. Similar results were obtained for the cationized forms of *cis*- and *trans*-fluoroproline. The drift profiles of $(M + Na)^+$ shows a 6.0 Å^2 Ω_{N2} difference and a $R_{p\text{-}p}$ = 0.84 (Figure 2e) between the diastereomers of fluoroproline compared to the 1.2 Å^2 difference and $R_{p\text{-}p}$ = 0.12 (Figure 2d) observed for the protonated ions. Adduction of multiple sodium ions does not result in a further improvement in $R_{p\text{-}p}$ (Figures 2c and f), indicating that the increase in resolution is not inherently a result of sodium ion attachment alone. These results indicate that sodium cationization stabilizes a unique and specific ion structure that is substantially different for each of these diastereomers.

Effect of Metal Ion Size on Diastereomer Resolution in TWIMS-MS. To investigate the effect of alkali metal ion size on diastereomer resolution using TWIMS-MS, ion mobility spectra for $[M + X]^+$, where X = Li, Na, K, and Cs, were obtained and compared to that observed for the protonated ions (Figure 3) of *cis*- and *trans*-hydroxyproline. In all cases, the metal ion cationized molecules showed a minimum of a factor of 4 increase in $R_{p\text{-}p}$ between the diastereomers compared to

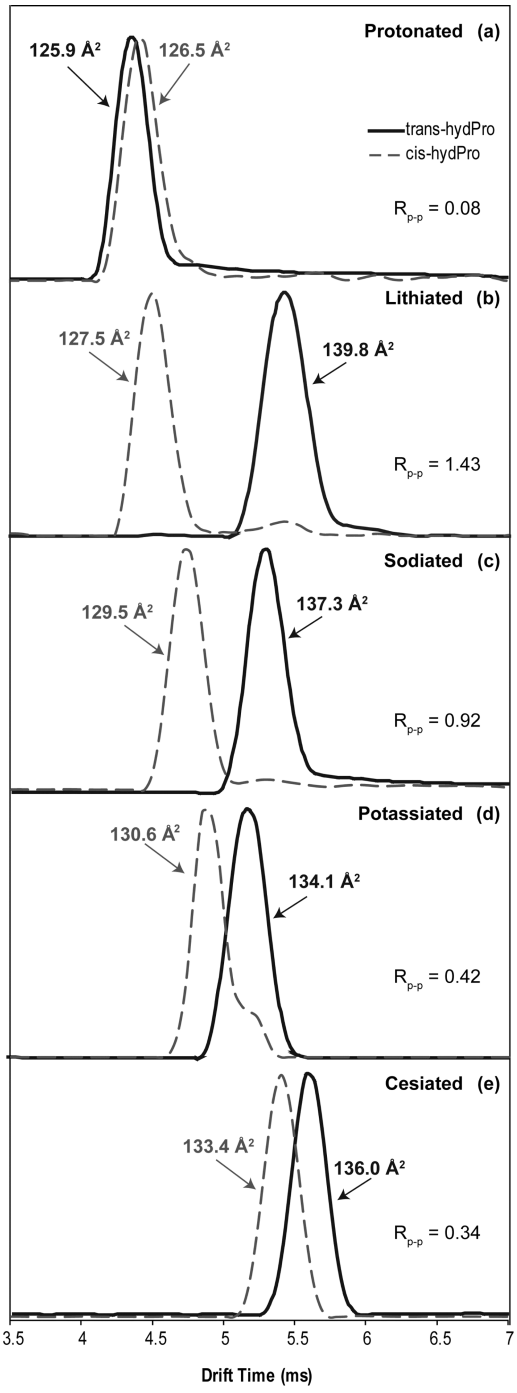

Figure 3. Traveling wave ion mobility spectra for (a) $[M + H]^+$ and $[M + X]^+$, where X = (b) Li, (c) Na, (d) K, or (e) Cs, for *cis*- and *trans*-hydroxyproline (hydPro) using N_2 as the drift gas.

the protonated counterparts. The most pronounced difference between drift times was observed for $[M + Li]^+$, where baseline separation was achieved, and the Ω_{N2} difference and $R_{p\text{-}p}$ observed between *cis*- and *trans*-hydroxyproline was 12.3 Å^2 and 1.43, respectively. The observed Ω_{N2} difference between diastereomers decreases from 12.3 to 2.6 Å^2 as the ionic radius of the alkali metal increases. Similar results were obtained for *cis*- and *trans*-fluoroproline (Figure S3). These results indicate that the metal ion size, or charge density, is a critical factor determining TWIM separation and therefore distinguishing the diastereomers in the gas phase.

DOI: 10.1021/ac5043285
Anal. Chem. 2015, 87, 3300−3307

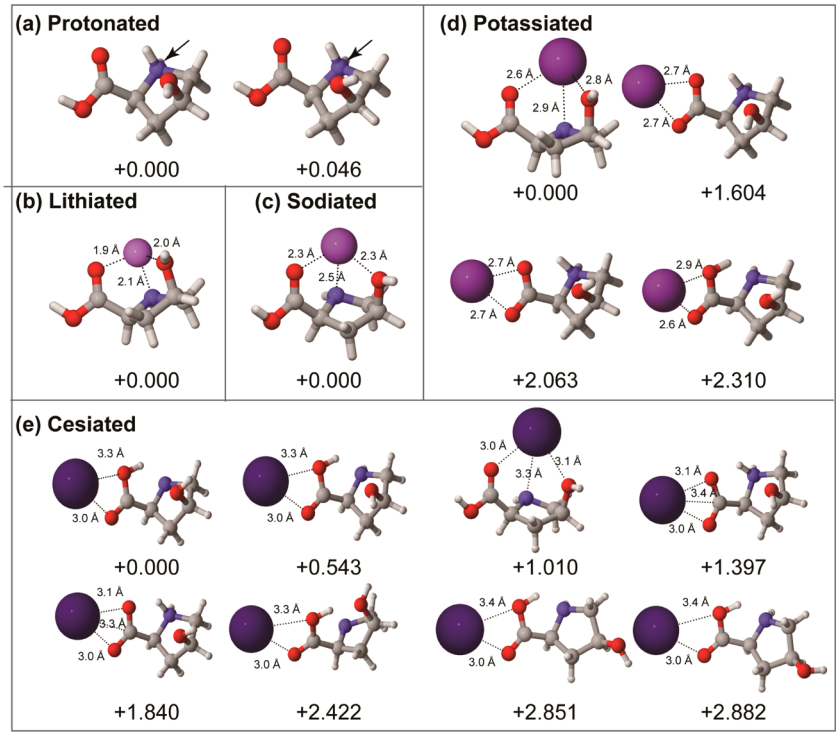

Figure 4. Lowest energy conformers possessing Gibbs free energy with 3 kcal mol^{-1} of the global energy minimum for (a) $[M + H]^+$ and $[M + X]^+$, where X = (b) Li, (c) Na, (d) K, or (e) Cs, for *cis*-hydroxyproline. In panel (a), the arrow denotes the site of protonation.

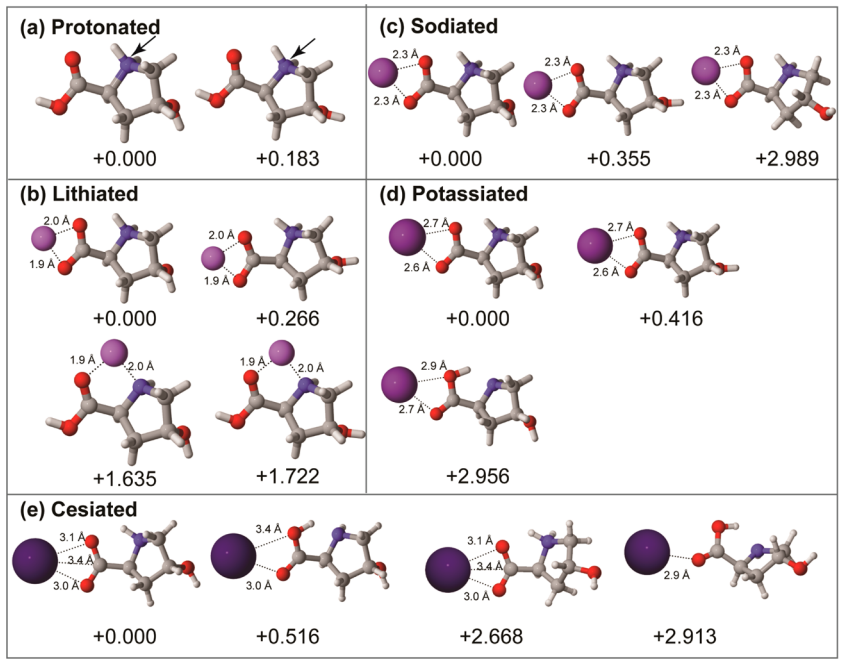

Figure 5. Lowest energy conformers possessing Gibbs free energy within 3 kcal mol^{-1} of the global free energy minimum for (a) $[M + H]^+$ and $[M + X]^+$, where X = (b) Li, (c) Na, (d) K, or (e) Cs, for *trans*-hydroxyproline. In panel (a), the arrow denotes the site of protonation.

Theoretical Structures of $[M + H]^+$ and $[M + X]^+$, where X = Li, Na, K, and Cs, for proline diastereomers. To investigate the relationship between experimental Ω_{N2} and the structure adopted by the diastereomers when protonated or metal cationized, all possible conformers of all possible cationized states were computed for $[M + H]^+$ and $[M + X]^+$, where X = Li, Na, K, or Cs, for *cis*- (Figure 4) and *trans*-hydroxyproline (Figure 5). Unique structures within a 3 kcal mol^{-1} Gibbs free energy window are depicted, with an expanded set (5 kcal mol^{-1} window) available in Figures S4 and S5. For both protonated *cis*- and *trans*-hydroxyproline, the ion exists predominantly in a structurally compact form with the proton residing on the nitrogen atom of the pyrrolidine ring. The two energetically similar conformers near the global minimum of $[M + H]^+$ result from slight differences in the orientation of the hydroxyl substituent on the pyrrolidine ring.

DOI: 10.1021/ac5043285
Anal. Chem. 2015, 87, 3300−3307

Table 1. Experimental and theoretical (Boltzmann-weighted) Ω_{N2} values for $[M + H]^+$ and $[M + X]^+$, where X = Li, Na, K, or Cs, for *cis*- and *trans*- hydroxyproline. All values are reported as Å^2

	cis-hydroxyproline		*trans*-hydroxyproline		*cis*-fluoroproline		*trans*-fluoroproline		*trans*-proline
charge carrier	exp.	theor.	exp.	theor.	exp.	theor.	exp.	theor.	theor.
H	126.5	120.7 ± 1.4	125.9	120.3 ± 1.5	126.6	121.3 ± 1.6	125.4	120.5 ± 1.2	117.8 ± 1.3
Li	127.5	120.0 ± 1.3	139.8	128.0 ± 1.4	127.2	120.1 ± 1.2	139.8	128.2 ± 1.2	124.2 ± 1.1
Na	129.5	122.8 ± 1.0	137.3	129.0 ± 1.6	130.1	123.4 ± 1.2	136.1	129.5 ± 1.6	125.1 ± 1.5
K	130.6	124.6 ± 1.1	134.1	129.6 ± 1.5	131	126.1 ± 1.2	134.5	130.2 ± 1.6	125.5 ± 1.5
Cs	133.4	129.4 ± 1.4	136.0	129.5 ± 1.5	133.4	129.9 ± 1.4	135.8	133.6 ± 1.5	126.9 ± 1.3

The highly similar overall topology of the dominant *cis* and *trans* $[M + H]^+$ (Figures 4a and 5a) is consistent with the minimal difference in experimentally observed Ω_{N2} values (Figures 2a and 3a).

In the case of the metalated systems, the lowest energy conformers of [*trans*-hydroxyproline + X]$^+$, where X = Li, Na, K, or Cs, exists in a nearly linear salt-bridge form,[47−56] involving metal complexation with the pendant carboxylate and protonation of the pyrrolidine N (Figure 5). The *trans* disposition of the hydroxyl function precludes its participation in metal binding. In contrast, the lowest energy conformer for [*cis*-hydroxyproline + X]$^+$, where X = Li, Na, or K, exists in a charge-solvated[47−56] structure, in which the acid carbonyl, hydroxyl group, and pyrrolidine ring all participate in encapsulation the metal ion, resulting in a tight, compact structure (Figure 4). These results are consistent with the smaller Ω_{N2} values (both TWIM and theoretically derived) obtained for metalated *cis*-hydroxyproline and the larger Ω_{N2} values obtained for metalated *trans*-hydroxyproline ions and demonstrate why baseline resolution was observed for these isomeric species when complexed with lithium and sodium alkali metal ions.

Unlike the series of *trans*-hydroxyprolines, the distribution of complexation states (and thus overall ion size and location of greatest positive charge) of the metalated *cis*-hydroxyproline changes significantly as the size of the alkali metal ion increases. While the linear salt-bridge form is not a competitive structure for the lithiated ion (ΔG > 5 kcal mol^{-1}), the linear salt-bridge forms of the sodiated and potassiated ions are found to reside 4.3 (Figure 8, Supporting Information) and 1.6 kcal mol^{-1}, respectively, above the corresponding compact charge-solvated form. In the case of [*cis*-hydroxyproline + Cs]$^+$, the trend is actually *reversed*; the linear form is now dominant and the charge-solvated encapsulated form resides about 1.0 kcal mol^{-1} higher in energy. Taken together, these results are consistent with the substantial increase in the experimental Ω_{N2} for *cis*-hydroxyproline as the size of the metal ion increases, whereas no significant change was observed in the experimental Ω_{N2} for *trans*-hydroxyproline with metal ion size, as the linear form is dominant for each. It is likely that increasing the size of the metal ion gives rise to greater steric congestion in the compact forms of metalated *cis*-hydroxyproline, ultimately preferring the linear form in the case of Cs$^+$. Similar trends as described here were observed for the theoretical structures of protonated and metal-cationized *cis*- and *trans*-fluoroproline and *trans*-proline (Figures S6, S7, and S8). The results presented here are consistent with IRMPD spectroscopy results that have shown that the stability of the salt-bridge form can be largely dependent on the size of the alkali metal ion.[51,55,56] Currently, this is the first report that shows that the charge-solvated and salt-bridged forms of amino acids can be clearly differentiated using TWIMS analysis.

In order to compare the theoretically calculated structures to the experimental Ω_{N2}, a theoretical Ω_{N2} was determined for each structure using an N_2-based TM algorithm, and a Boltzmann-weighted theoretical Ω_{N2} was determined based on the contributing population of each structure. The resultant Boltzmann-weighted theoretical Ω_{N2} was then compared to the experimental Ω_{N2} (Table 1). The theoretical Ω_{N2} shows close agreement with experimental Ω_{N2}. Both theoretically and experimentally, little difference in Ω_{N2} was observed for the protonated ions of *cis*- and *trans*-hydroxyproline, and the biggest difference in Ω_{N2} was observed for the lithiated ion. Similarly, the theoretical and experimental Ω_{N2} for [*cis*-hydroxyproline + X]$^+$, where X = Li, Na, K, or Cs, both increase with metal ion size, providing further evidence of the transition from the compact charge-solvated form to the linear salt-bridge structure for the *cis*- isoform as the size of the metal ion increases.

Relating the Ion's Charge Distribution to Its Observed IM Separation. Recent results have demonstrated that more polarizable drift gases[19,63] can be used to improve diastereomer and other structurally related compounds using TWIMS analysis when a significant difference in the dipole moment value exists between the two ionic species. The calculated dipole moments (μ) for all species in this study are provided in Table S1. Panels (a) and (b) of Figure 6 depict the electrostatic potential mapped upon the electron density surfaces of lithiated *cis*- and *trans*-hydroxyproline, respectively, along with the corresponding atomic charges based on the ESP fit. These two lithiated diastereomers were found to exhibit the greatest difference in computed dipole moment among all the metal−chelated species ($\Delta\mu$ = 1.38 D). For lithiated *cis*-hydroxyproline (μ = 2.07 D), the positive region in the vicinity of the Li atom is encapsulated by the nearby regions of relative negative charge due to the chelating heteroatoms. Conversely, the *trans* orientation of the pendant, noncomplexing hydroxyl group in *trans*-hydroxyproline (μ = 3.45 D) gives rise to a greater separation of charge and resultant dipole moment than the *cis* form.

In order to determine if the difference in dipole moment can be exploited to improve the resolution of these diastereomers by using a different drift gas, ion mobility spectra of $[M + Li]^+$ for *cis*- and *trans*-hydroxyproline were obtained using CO_2 (Figure 6c), N_2 (Figure 6d), or He (Figure 6e) as the drift gas. Performing this analysis on an RF-confining drift cell instrument provided many advantages. For example, the pressure of each drift gas could be measured accurately; therefore, a constant pressure (1.5 Torr) for all measurements could be achieved allowing for accurate ion mobility spectra comparisons between drift gases (He, N_2, and CO_2). Accurate Ω measurements could also be derived in each gas; this would have been impossible for CO_2 on the TWIMS instrument because there are no CO_2 calibration standard values. When

DOI: 10.1021/ac5043285
Anal. Chem. 2015, 87, 3300−3307

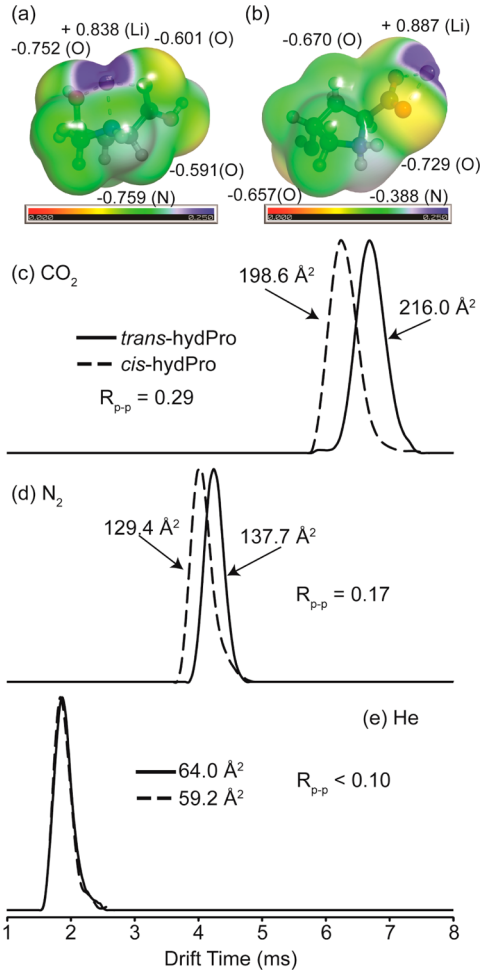

Figure 6. Isosurfaces (at the 0.001 au contour level) depicting the B3LYP/6-31++G(d,p) electrostatic surface potential mapped onto the total electron density for (a) [*cis*-hydroxyproline + Li]$^+$ and (b) [*trans*-hydroxyproline + Li]$^+$ with corresponding atomic charges. Isosurface value coloration: blue, positive; red, negative. Ion mobility spectra obtained on an RF-confining drift cell instrument for lithiated *cis*- and *trans*-hydroxyproline using (c) CO_2, (d) N_2, or (e) He as the drift gas. RF-confining drift cell voltage gradient of 135 V and a pressure of 1.5 Torr.

using He, an insignificant difference between the *cis*- and *trans*-forms is observed ($R_{p\text{-}p} < 0.1$) with a small but measurable Ω_{He} difference (4.8 Å^2). The observed resolution between the diasteromers is significantly improved when N_2 is used as the drift gas ($R_{p\text{-}p} = 0.17$) corresponding to an increased Ω_{N2} difference (8.3 Å^2), but the greatest improvement in resolution is observed with CO_2 ($R_{p\text{-}p} = 0.29$ and Ω_{CO2} difference of 17.4 Å^2), the drift gas with the highest polarizability constant. This improvement in the $R_{p\text{-}p}$ value is also observed on the TWIMS instrument (Figure S9). Further discussion on the effect of the ion's dipole moment on the drift time and how this correlates to the theoretical Ω derived from the projection approximation (PA) algorithm can be found in the Supporting Information.

A relationship between the predicted dipole moment and Ω is also observed for the additional cationized (Li, Na, K, and Cs) species analyzed within this study, where the dipole moment value is found to be higher for all *trans*-hydroxyproline metal-chelated species except for cesium. For the lithiated hydroxyproline ions that display the greatest TWIM separation ($R_{p\text{-}p}$ 1.43; Figure 3b), these ions also possess the largest $\Delta\mu$ (1.38 D). The TWIM separation of the sodiated species is lower ($R_{p\text{-}p} = 0.92$; Figure 3c), corresponding to the lower $\Delta\mu$ value (0.98 D). TWIM separation is further reduced for the potassiated species ($R_{p\text{-}p} = 0.42$; Figure 3d), possessing a $\Delta\mu$ of 0.42 D. The cesiated hydroxyproline ions are analogous to the protonated *cis* and *trans*-hydroxyproline species, in that the *cis*-form possesses a larger dipole moment value (2.94 D) than the *trans*- form (1.78 D). As the chelated metal ion increases in size, the drift time of the *cis*-hydroxyproline increases (less mobile) due to the increased long-range charge induced dipole attractive forces between the ion and the neutral drift gas, whereas the drift time of the *trans*- form remains fairly constant. These TWIMS observations for the metal-cationized ions can also be rationalized as a function of where the metal ion resides on the hydroxyproline molecule (*vida supra*). These results further demonstrate that the charge distribution on the ionic species can result in both subtle and dramatic drift time differences and also that more polarizable drift gases (than He) can be used to improve isomeric resolution when the isomeric pair's dipole moments significantly differ.

CONCLUSIONS

Results presented here indicate that alkali metal ion cationization substantially improves the resolution between isomeric proline variants in TWIMS analysis. The experimental Ω_{N2} are in excellent agreement with those determined theoretically. The improvement in TWIMS separation for the isomeric proline molecules can be attributed to a combination of the *trans*- form adopting a linear, salt-bridge structure, whereas the *cis*- form exists primarily in a compact, charge-solvated form for small alkali metal ions, and also the effect of the charge distribution of the ion and its effect on the long-range charge induced dipole interaction with the neutral drift gas. The results demonstrate the first example illustrating the capability for TWIMS analysis to distinguish a salt-bridge vs charge-solvated gas-phase structure for an amino acid. Also, these results indicate that smaller alkali metal ions, such as lithium, may provide an analytical advantage in TWIMS analysis for isomeric resolution. A recent study[14] also demonstrated the importance of alkali metal cationization in isomeric resolution but did not probe the relationship between resolution behavior and the structural role of the cation, a key focal point of the current work. The ability of small alkali metal ions to improve isomer resolution for TWIMS (and RF-confining drift cell) analysis can potentially be used for many different applications, such as for both small molecule and protein- or peptide-based therapeutics. However, it is critical that adduction of the alkali metal ion to the isoforms is capable of stabilizing a gas-phase structure that is unique, or at least preferential, to only one isomer. As our understanding progresses of how alkali metal ions adduct to different amino acids and small molecules in the gas phase, the capability of alkali metal ions as a tool to improve isoform resolution in TWIMS analysis will have greater utility.

ASSOCIATED CONTENT

Supporting Information

Additional information as noted in text. This material is available free of charge via the Internet at http://pubs.acs.org.

AUTHOR INFORMATION

Corresponding Author

*Phone: (805) 447-0143. E-mail: tflick@amgen.com.

DOI: 10.1021/ac5043285
Anal. Chem. 2015, 87, 3300−3307

Notes

The authors declare no competing financial interest.

■ ACKNOWLEDGMENTS

The authors gratefully acknowledge Kevin Giles and Mike Morris from the Waters Corporation, MS Technologies, Manchester, U.K., for providing the hardware and technical advice that allowed us to upgrade our TWIM instrument to an RF-confining drift cell instrument.

■ REFERENCES

(1) Hely, M.; Morris, J.; Traficante, R.; Reid, W.; O'Sullivan, D.; Williamson, P. *J. Neurol., Neurosurg. Psychiatry* **1999**, *67*, 300.
(2) Fabro, S. S.; R.L; Williams, R. T. *Nature* **1967**, *215*, 296.
(3) Shapira, R.; Wilkinson, K. D.; Shapira, G. *Prog. Clin. Biol. Res.* **1989**, *292*, 487.
(4) Buczek, O.; Yoshikami, D.; Bulaj, G.; Jimenez, E. C.; Olivera, B. M. *J. Biol. Chem.* **2005**, *280*, 4247.
(5) Kreil, G. *Annu. Rev. Biochem.* **1997**, *66*, 337.
(6) Wu, C.; Siems, W. F.; Klasmeier, J.; Hill, H. H., Jr. *Anal. Chem.* **2000**, *72*, 391.
(7) Counterman, A. E.; Clemmer, D. E. *Anal. Chem.* **2002**, *74*, 1946.
(8) Pierson, N. A.; Chen, L.; Russell, D. H.; Clemmer, D. E. *J. Am. Chem. Soc.* **2013**, *135*, 3186.
(9) Dale, J. A.; Mosher, H. S. *J. Am. Chem. Soc.* **1973**, *95*, 512.
(10) Roussel, C.; Del Rio, A.; Pierrot-Sanders, J.; Piras, P.; Vanthuyne, N. *J. Chromatogr. A* **2004**, *1037*, 311.
(11) Scriba, G. K. E. *Bioanal. Rev.* **2011**, *3*, 95.
(12) Yamagaki, T.; Sato, A. *Anal. Sci.* **2009**, *25*, 985.
(13) Li, H.; Giles, K.; Bendiak, B.; Kaplan, K.; Siems, W. F.; Hill, H. H., Jr. *Anal. Chem.* **2012**, *84*, 3231.
(14) Domalain, V.; Tognetti, V.; Hubert-Roux, M.; Lange, C. M.; Joubert, L.; Baudoux, J.; Rouden, J.; Afonso, C. *J. Am. Soc. Mass Spectrom.* **2013**, *24*, 1437.
(15) McCooeye, M.; Ding, L.; Gardner, G. J.; Fraser, C. A.; Lam, J.; Sturgeon, R. E.; Mester, Z. *Anal. Chem.* **2003**, *75*, 2538.
(16) Barnett, D. A.; Ells, B.; Guevremont, R.; Purves, R. W. *J. Am. Soc. Mass Spectrom.* **1999**, *10*, 1279.
(17) Barnett, D. A.; Purves, R. W.; Ells, B.; Guevremont, R. *J. Mass Spectrom.* **2000**, *35*, 976.
(18) Clowers, B. H.; Dwivedi, P.; Steiner, W. E.; Hill, H. H., Jr.; Bendiak, B. *J. Am. Soc. Mass Spectrom.* **2005**, *16*, 660.
(19) Lalli, P. M.; Corillo, Y. E.; Fasciotti, M.; Riccio, M. F.; de Sa, G. F.; Daroda, R. J.; Souza, G. H. M. F.; McCullagh, M.; Bartberger, M. D.; Eberlin, M. N.; Campuzano, I. D. G. *J. Mass Spectrom.* **2013**, *48*, 989.
(20) Asbury, G. R.; Hill, H. H., Jr. *Anal. Chem.* **2000**, *72*, 580.
(21) Leavell, M. D.; Gaucher, S. P.; Leary, J. A.; Taraszka, J. A.; Clemmer, D. E. *J. Am. Soc. Mass Spectrom.* **2002**, *13*, 284.
(22) Wu, L.; Cooks, R. G. *Anal. Chem.* **2003**, *75*, 678.
(23) Zhang, D.; Tao, W. A.; Cooks, R. G. *Int. J. Mass Spectrom.* **2001**, *204*, 159.
(24) Grigorean, G.; Ramirez, J.; Ahn, S. H.; Lebrilla, C. B. *Anal. Chem.* **2000**, *72*, 4275.
(25) Green, M. K.; Lebrilla, C. B. *Mass Spectrom. Rev.* **1997**, *16*, 53.
(26) Grigorean, G.; Lebrilla, C. B. *Anal. Chem.* **2001**, *73*, 1684.
(27) Dang, T. T.; Pederson, S. F.; Leary, J. A. *J. Am. Soc. Mass Spectrom.* **1994**, *5*, 452.
(28) Dearden, D. V.; Chadin, D.; Liang, Y.; Bradshaw, J. S.; Izatt, R. M. *J. Am. Chem. Soc.* **1997**, *119*, 353.
(29) Ramirez, J.; He, F.; Lebrilla, C. B. *J. Am. Chem. Soc.* **1998**, *120*, 7387.
(30) Baker, E. S.; Hong, J. W.; Gidden, J.; Bartholomew, G. P.; Bazan, G. C.; Bowers, M. T. *J. Am. Chem. Soc.* **2004**, *126*, 6255.
(31) Campuzano, I. D. G.; Bush, M. F.; Robinson, C. V.; Beaumont, C.; Richardson, K.; Kim, H.; Kim, H. I. *Anal. Chem.* **2012**, *84*, 1026.
(32) Domalain, V.; Hubert-Roux, M.; Lange, C. M.; Baudoux, J.; Rouden, J.; Afonso, C. *J. Mass Spectrom.* **2014**, *49*, 423.
(33) Dwivedi, P.; Wu, C.; Matz, L. M.; Clowers, B. H.; Siems, W. F.; Hill, H. H., Jr. *Anal. Chem.* **2006**, *78*, 8200.
(34) Lalli, P. M.; Iglesias, B. A.; Deda, D. K.; Toma, H. E.; de Sa, G. F.; Daroda, R. J.; Araki, K.; Eberlin, M. N. *Rapid Commun. Mass Spectrom.* **2011**, *26*, 263.
(35) Matz, L. M.; Hill, H. H., Jr.; Beegle, L. W.; Kanik, I. *J. Am. Soc. Mass Spectrom.* **2002**, *13*, 300.
(36) Matz, L. M.; Hill, H. H., Jr. *Anal. Chem.* **2001**, *73*, 1664.
(37) Williams, J. P.; Bugarcic, T.; Habtemariam, A.; Giles, K.; Campuzano, I. D.G.; Rodger, P. M.; Sadler, P. J. *J. Am. Soc. Mass Spectrom.* **2009**, *20*, 1119.
(38) Dwivedi, P.; Wu, C.; Matz, L. M.; Clowers, B. H.; Siems, W. F.; Hill, H. H., Jr. *Anal. Chem.* **2006**, *78*, 8200.
(39) Wyttenbach, T.; Witt, M.; Bowers, M. T. *J. Am. Chem. Soc.* **2000**, *122*, 3458.
(40) Clemmer, D. E.; Jarrold, M. F. *J. Mass Spectrom.* **1997**, *32*, 577.
(41) Baumketner, A.; Bernstein, S. L.; Wyttenbach, T.; Bitan, G.; Teplow, D. B.; Bowers, M. T.; Shea, J. E. *Protein Sci.* **2006**, *15*, 420.
(42) Uetrecht, C.; Rose, R. J.; van Duijn, E.; Lorenzen, K.; Heck, A. J. R. *Chem. Soc. Rev.* **2010**, *39*, 1633.
(43) Ruotolo, B. T.; Hyung, S. J.; Robinson, P. M.; Giles, K.; Bateman, R. H.; Robinson, C. V. *Angew. Chem., Int. Ed.* **2007**, *46*, 8001.
(44) Loo, J. A.; Berhane, B.; Kaddis, C. S.; Wooding, K. M.; Xie, Y.; Kaufman, S. L.; Chernushevich, I. V. *J. Am. Soc. Mass Spectrom.* **2005**, *16*, 998.
(45) Giles, K.; Williams, J. P.; Campuzano, I. *Rapid Commun. Mass Spectrom.* **2011**, *25*, 1559.
(46) Kemper, P. R.; Dupuis, N. F.; Bowers, M. T. *Int. J. Mass Spectrom.* **2009**, *287*, 46.
(47) Oomens, J.; Steill, J. D.; Redlich, B. *J. Am. Chem. Soc.* **2009**, *131*, 4310.
(48) Heaton, A.; Bowman, V.; Oomens, J.; Steill, J.; Armentrout, P. *J. Phys. Chem. A* **2009**, *113*, 5519.
(49) Dunbar, R. C.; Hopkinson, A. C.; Oomens, J.; Siu, C.-K.; Siu, K. W. M.; Steill, J. D.; Verkerk, U. H.; Zhao, J. *J. Phys. Chem. B* **2009**, *113*, 10403.
(50) Polfer, N. C.; Oomens, J. *Mass Spectrom. Rev.* **2009**, *28*, 468.
(51) Bush, M. F.; Forbes, M. W.; Jockusch, R. A.; Oomens, J.; Polfer, N. C.; Saykally, R. J.; Williams, E. R. *J. Phys. Chem. A* **2007**, *111*, 7753.
(52) Drayss, M. K.; Blunk, D.; Oomens, J.; Schäfer, M. *J. Phys. Chem. A* **2008**, *112*, 11972.
(53) Fridgen, T. D. *Mass Spectrom. Rev.* **2009**, *28*, 586.
(54) Bush, M. F.; Campuzano, I. D. G.; Robinson, C. V. *Anal. Chem.* **2012**, *84*, 7124.
(55) Jockusch, R. A.; Lemoff, A. S.; Williams, E. R. *J. Am. Chem. Soc.* **2001**, *123*, 12255.
(56) Strittmatter, E. F.; Lemoff, A. S.; Williams, E. R. *J. Phys. Chem. A* **2000**, *104*, 9793.
(57) *Molecular Operating Environment (MOE)*; Chemical Computing Group, Inc.: Montreal, QC, Canada, 2013.
(58) Rappoport, D.; Furche, F. *J. Chem. Phys.* **2010**, *133*, 134105.
(59) Singh, U. C.; Kollman, P. A. *J. Comput. Chem.* **1984**, *5*, 129.
(60) Frisch, M. J.; Trucks, G. W.; Schlegel, H. B.; Scuseria, G. E.; Robb, M. A.; Cheeseman, J. R.; Scalmani, G.; Barone, V.; Mennucci, B.; Petersson, G. A.; Nakatsuji, H.; Caricato, M.; Li, X.; Hratchian, H. P.; Izmaylov, A. F., Bloino, J., Zheng, G., Sonnenberg, J. L., Hada, M., Ehara, M., Toyota, K., Fukuda, R., Hasegawa, J., Ishida, M., Nakajima, T., Honda, Y., Kitao, O., Nakai, H., Vreven, T., Montgomery, J. A., Jr., Peralta, J. E., Ogliaro, F., Bearpark, M., Heyd, J. J.,Brothers, E., Kudin, K. N., Staroverov, V. N., Keith, T.,Kobayashi, R.,Normand, J., Raghavachari, K., Rendell, A., Burant, J. C., Iyengar, S. S., Tomasi, J., Cossi, M., Rega, N., Millam, J. M., Klene, M., Knox, J. E., Cross, J. B., Bakken, V.,Adamo, C., Jaramillo, J., Gomperts, R., Stratmann, R. E., Yazyev, O., Austin, A. J., Cammi, R., Pomelli, C., Ochterski, J. W., Martin, R. L.,Morokuma, K., Zakrzewski, V. G., Voth, G. A., Salvador, P.,Dannenberg, J. J., Dapprich, S., Daniels, A. D., Farkas, O., Foresman, J. B., Ortiz, J. V.,Cioslowski, J., Fox, D. J. *Gaussian 09, Rev. D.01*; Gaussian, Inc.: Wallingford, CT, 2013.

DOI: 10.1021/ac5043285
Anal. Chem. 2015, 87, 3300−3307

(61) Mesleh, M. F.; Hunter, J. M.; Shvartsburg, A. A.; Schatz, G. C.; Jarrold, M. F. *J. Phys. Chem.* **1996**, *100*, 16082.
(62) Rappe, A. K.; Casewit, C. J.; Colwell, K. S.; Goddard, W. A., III; Skiff, W. M. *J. Am. Chem. Soc.* **1992**, *114*, 10024.
(63) Lapthorn, C.; Dines, T. J.; Chowdhry, B. Z.; Perkins, G. L.; Pullen, F. S. *Rapid Commun. Mass Spectrom.* **2013**, *27*, 2399.

DOI: 10.1021/ac5043285
Anal. Chem. 2015, 87, 3300−3307